ELSEVIER

Plasmonics in composite nanostructures

Hong Wei[1,*] and Hongxing Xu[1,2,*]

[1] Beijing National Laboratory for Condensed Matter Physics and Institute of Physics, Chinese Academy of Sciences, Beijing 100190, China
[2] Center for Nanoscience and Nanotechnology, and School of Physics and Technology, Wuhan University, Wuhan 430072, China

Plasmonics is a rapidly developing research field with many potential applications in fields ranging from bioscience, information processing and communication to quantum optics. It is based on the generation, manipulation and transfer of surface plasmons (SPs) that have the ability to manipulate light at the nanoscale. Realizing plasmonic applications requires understanding how the SP-based properties depend on the nanostructures and how these properties can be controlled. For that purpose composite nanostructures are particularly interesting because many novel and extraordinary properties unattainable in single nanostructures can be obtained by designing composite nanostructures with various materials. Here, we review recent advances in the studies of three classes of composite nanostructure that are important for plasmonics: metal–metal, metal–dielectric, and metal–semiconductor composite nanostructures.

Introduction

With the development of nanoscience and nanotechnology, various nanostructures based on different materials can be fabricated in controllable ways. Among these, composite nanostructures have been intensively studied because many novel properties unattainable in single nanostructures can be obtained. Particularly, composite nanostructures are widely used in plasmonics, a booming research field aiming at the manipulation of light at the nanoscale. Plasmonics is based on the excitation of surface plasmons (SPs) – collective oscillations of free electrons at metal–dielectric interfaces, which can confine electromagnetic (EM) field at the metal's surface enabling light manipulation beyond the diffraction limit of light [1]. Most researches in plasmonics are within the visible and near infrared spectral regions, whereas some studies, noticeably those on plasmonic metamaterials, have extended plasmonics to the THz wave and microwave regions [2–6]. The plasmonic properties of metal nanostructures are strongly dependent on the geometrical parameters, the materials and the surrounding media of the nanostructures, which makes composite nanostructures extremely important in plasmonics to realize highly tunable and designable optical properties.

*Corresponding authors:. Wei, H. (weihong@iphy.ac.cn), Xu, H. (hxxu@iphy.ac.cn)

Based on the excitation of SPs, metal nanostructures show many prominent optical properties, for example, huge EM field enhancement, supersensitive plasmon resonance and propagation at the nanoscale. The huge EM field enhancement can be obtained in close-packed metal nanostructures, where the SP resonances can tightly confine EM field into tiny gaps due to the strong EM coupling of two metal surfaces, similar to the strong EM resonance in a cavity [7,8]. This effect enables the amplification of weak light–matter interactions, and is the basis for many very important research directions in plasmonics, including nanogap or ''hot spots'' for surface-enhanced Raman scattering (SERS) [7–10], optical antenna [11,12], plasmonic optical forces [13,14], plasmochemistry [15], quantum plasmonics [16,17] and nonlinear plasmonics [18,19]. For super sensitivity, the SP resonance frequencies are extremely sensitive to the change of the surrounding dielectric environment of the metal nanostructures, which has been used to develop ultrasensitive sensors [20]. For propagation at nanoscale, SPs can propagate in one-dimensional nanostructures with EM field tightly confined around the nanostructure, which can be used to realize light transmission beyond the diffraction limit and build nanophotonic circuits [21,22]. Because of these properties, plasmonics has shown potential applications in many fields, such as biological and chemical sensing [7,20], disease

1369-7021/ http://dx.doi.org/10.1016/j.mattod.2014.05.012

diagnosis and therapy [23–25], information processing and communication [21,22,26], quantum optics [27], photovoltaics [28], catalysis [15,29,30], lithography and imaging [31–33].

The tailoring of the plasmonic properties for implementation in these applications relies on the design and fabrication of composite nanostructures. It is therefore essential to investigate the properties of such composite plasmonic nanostructures to understand how the composite nanostructures determine their specific plasmon-related properties. Here we briefly review recent advances in studying three classes of composite plasmonic nanostructures: metal–metal, metal–dielectric, and metal–semiconductor composite nanostructures.

Metal–metal composite nanostructures

Here the metal–metal composite nanostructures mean the nanostructures composed of two or more metal nanostructure components, not the alloy nanostructures. As the SP resonance frequencies of gold and silver nanostructures are at visible and near infrared spectral range, gold and silver are the most popular metal materials used in plasmonics. Due to SP resonance, single metal nanoparticles (NP) are able to concentrate EM energy, leading to locally enhanced EM field near the NP [34]. This effect can be enhanced in systems where metal nanoparticles (NPs) are brought into close proximity to another metal structure. For a dimer consisting of two metal nanoparticles, the coupling between the localized SP modes will strengthen the EM field in the interparticle nanogap and red-shift the resonance frequency for incident polarization along the dimer axis [7,8], which can be theoretically described by the coupling of two dipoles. Although decreasing the separation between two coupled metal nanostructures can increase the electric field intensity and red-shift the resonance frequency, an extreme decrease in the separation to the dimension of angstrom scale can decrease the enhancement factor and blue-shift the SP resonance frequency due to quantum effects [16,17,35,36].

The large EM field enhancement in the nanogaps (also called the nanogap effect) is the most pronounced phenomenon in metal–metal composite nanostructures, which leads to many plasmon-enhanced phenomena. The nanogap with enhanced EM field becomes the 'hot spot' for SERS and surface-enhanced fluorescence [7,8,37–39]. The EM enhancement has been employed to enhance some nonlinear optical processes such as high-harmonic generation and four-wave mixing [19,40]. Lasing has been reported to occur around EM hot spots in Au bow-tie-shaped NPs supported by an organic gain material [41]. The hot spots can also enhance optical forces, which can be used for trapping NPs and molecules [13,14,42–44]. Composite metal nanostructures can function as antennas to modulate the polarization and direction of emitted light, which provides large flexibility for light manipulation at the nanoscale [11,12,45,46]. Recently, plasmon-enhanced chemical reactions have drawn much attention. The hot electrons generated by SP resonances assist the occurrence of some chemical reactions, for example dimerizing 4-nitrobenzenethiol to dimercaptoazobenzene [15,30].

As SPs are strongly dependent on the geometry of nanostructures, metal–metal composite nanostructures of various geometries have been investigated [47]. Besides Au–Au and Ag–Ag composite nanostructures, heterometal structures of Au–Ag have also been studied for tuning SP resonances and routing light of different colors [48,49]. The EM coupling in composite metal nanostructures is strongly dependent on the structure configuration, which offers a unique strategy to tune the optical properties [50,51]. For example, end-to-end aligned gold nanorods show red-shifted SP resonance compared to single nanorod, while side-by-side gold nanorods show blue-shifted SP resonance. In composite structures of specific configurations, the interference of different SP modes results in Fano resonances and electromagnetically induced transparency, which have sharp resonance features and may be used for ultrasensitive sensing [52–54].

Hot spots for surface-enhanced Raman scattering (SERS)

Raman spectroscopy is an important technique for detecting and analyzing molecules with the molecular ''fingerprints'' contained in the spectra. But the Raman signals of molecules are usually very weak due to the small scattering cross sections, which limits the sensitivity of the Raman spectroscopy for detecting analytes. SERS greatly improves the sensitivity of Raman by using the field enhancement effect of metal nanostructures. The huge EM field enhancement in the nanogaps, that is, hot spots, of metal composite nanostructures can enhance the Raman intensity by a few orders. Nanoparticle dimers are the simplest composite structures that contain such nanogaps. Actually, the large EM field enhancement in the nanogap was first revealed in the study of single-molecule SERS [7,8]. The scanning electron microscopy (SEM) image in Fig. 1a shows a dimer of Ag NPs, which was used to detect the SERS signal of single hemoglobin molecules. The EM coupling strength strongly depends on the separation of the two particles and the polarization of excitation light. From the calculated electric field distributions in Fig. 1a, it can be seen that the highest EM field is obtained with polarization parallel to the dimer axis due to the two induced dipoles in NPs strengthening each other. For perpendicular polarization, no enhancement is generated in the nanogap as the two dipoles cancel each other [55].

Apart from dimers of two nanospheres, dimers composed of nanospheres and other structures can also generate hot spots (Fig. 1b–d shows three types of asymmetrically coupled structures). For example, by placing an Au NP into a nanosized hole in an Au film, a hole–particle pair is formed (Fig. 1b). The hole–particle nanogap provides a large-volume hot spot that gives rise to a strongly enhanced Raman signal for molecules located in the nanogap [56]. A second example of a structure in which such a hot-spot is formed is the junction between a nanowire (NW) and an adjacent NP (Fig. 1c) [57]. Because the NW can function as a waveguide for SPs, the hot spot at the NW–NP junction can be remotely excited by focusing the excitation light at one end of the NW [58]. Finally, the EM coupling between a metal NP and a metal film can also generate a hot spot in the nanogap formed between them (Fig. 1d). The ease-of-fabrication of this type of structure makes it a good candidate for SERS substrate [59]. We note that the apex of a metal tip on scanning probe microscope can be regarded as a controllable nanoparticle. By coupling the tip with a metal film or a metal nanoparticle on the film, nanogap can be controllably created. Tip-enhanced Raman spectroscopy (TERS) has been developed based on the hot-spots in the tip-substrate coupled structures [15,60–63].

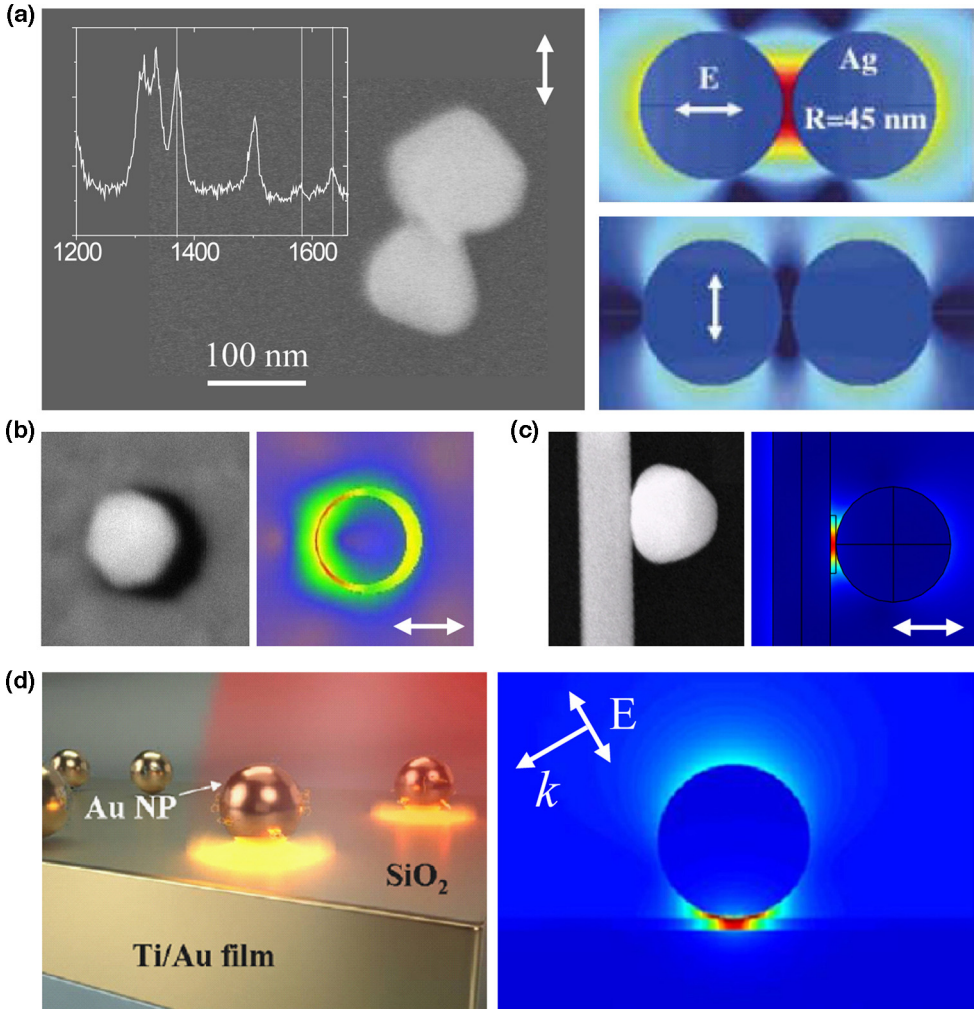

FIGURE 1

Four types of metal–metal composite nanostructures. (a) SEM image of an Ag NP dimer (left) and the calculated electric field intensity distributions for two polarizations (right). (b) and (c) SEM images (left) of nanohole–nanoparticle and nanowire–nanoparticle composite structures, and the calculated electric field intensity distributions (right). (d) Schematic structure of Au NPs deposited on an Au mirror coated with a thin dielectric layer (left) and the calculated electric field intensity distribution (right). The double-headed arrows indicate the polarizations of excitation light. Adapted from Ref. [7,55–57,59].

Metal nanowire networks for SP guiding and routing

One-dimensional metal nanostructures can support propagating SPs to realize the light guiding beyond the diffraction limit. They can thereby function as the subwavelength counterparts to optical fibers to be used as potential building blocks for integrated plasmonic circuitry [21,22]. Many structures have been proposed as plasmonic waveguides [64–67]; among these, chemically synthesized metal NWs show superior performances due to their crystalline structure which results in low propagation loss [67,68]. Intensive studies into SP propagation on individual metal NWs have been performed, which reveals the fundamental properties of nanowire SPs, for example the emission direction, propagation loss and group velocity of SPs [22,69]. Complex NW structures and networks can be built by assembling individual metal NWs. The control of SP propagation in nanowire-based composite structures and networks is an important step toward manipulating light transmission in functional and complicated nanophotonic circuits.

The propagation of SPs in such one-dimensional composite structures and the output therefrom can be controlled by tuning the input polarization. The propagating SPs excited at one end of the NW can be converted into photons at the output end of the NW as well as a metal NP placed in proximity to the NW waveguide (Fig. 2ai,aii). This is because the scattering at these discontinuities can compensate the momentum mismatch between SPs and photons. The intensity of the scattered light at the particle position is dependent on the polarization of the excitation light (Fig. 2aii,aiv). To understand the polarization-dependent scattering of the nanoparticle, the near-field distributions of the propagating SPs were imaged by using the fluorescence of quantum dots (QDs) on the sample surface (Fig. 2aiii,av). As the QD fluorescence is excited by the propagating SPs, the QD fluorescence intensity corresponds to the electric field intensity of SPs on the NW [70,71]. This near-field distribution is also dependent on the polarization of the input light (Fig. 2aiii,av). These results show that scattering intensity at the NW–NP junction is determined by the near-field intensity at the junction. For the polarization in Fig. 2aii,aiii, the near-field intensity at the NW–NP junction is strong, which leads to strongly scattered light at the junction. For the polarization shown in Fig. 2aiv, av, the near field at the junction is weak.

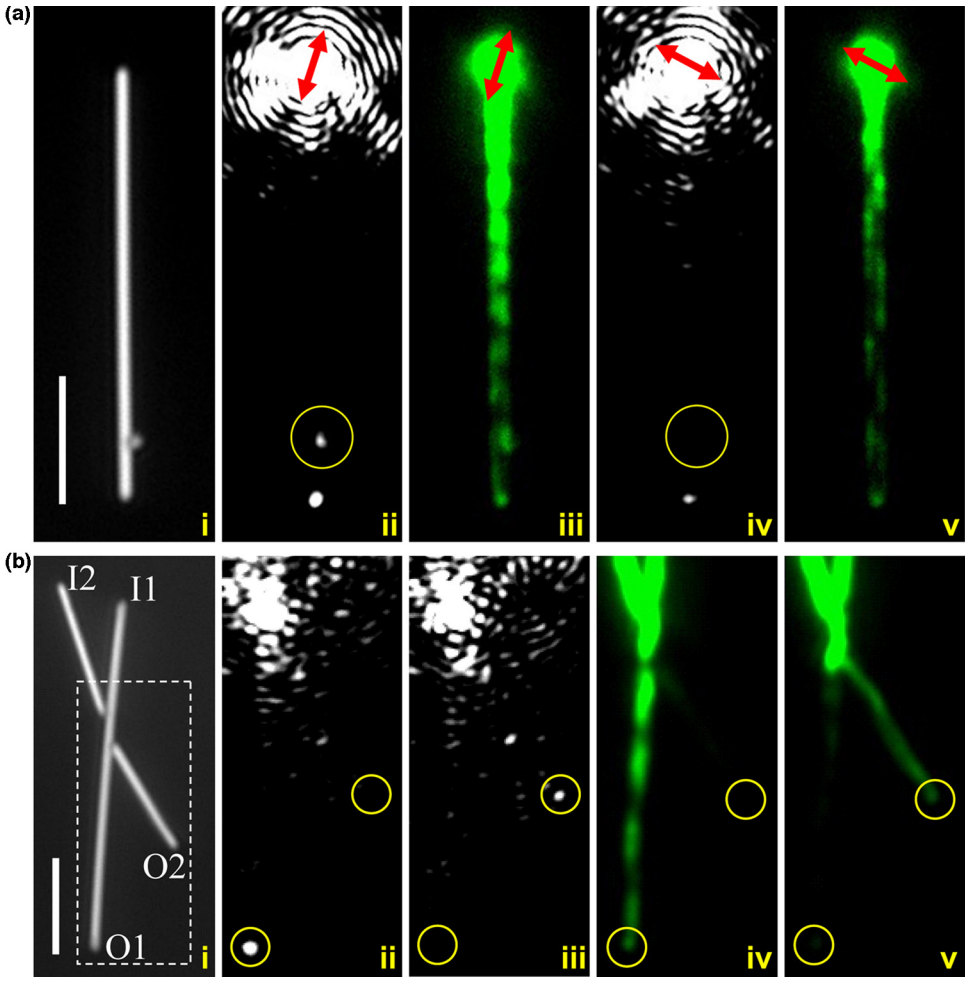

FIGURE 2

Composite metal nanostructures based on Ag NWs that support propagating SPs. (a) i: White-light optical image of a NW–NP structure. ii, iv: Scattering images for laser light of different polarizations focused on the top end of the NW. iii, v: Images of QD fluorescence revealing the distribution of near-field intensity. (b) i: White-light optical image of a NW network. ii, iii: Scattering images for interference of two SP beams. iv, v: Images of QD fluorescence corresponding to ii and iii, respectively. The dashed rectangle in (i) outlines the area displayed in (ii) to (v). The scale bars represent 5 μm. The NW radius is about 150 nm. Adapted from Ref. [71].

Therefore, there is almost no detectable scattering at the junction. The distribution of the near field determines if the SPs on the NW can be routed to other structures connected to the wire. For example, if the NP is replaced by a NW, a branched nanowire system is formed. By tuning the polarization of the input light, SPs in such a system can be controllably routed to different output terminals, which makes the branched nanowire a router for signal control in integrated plasmonic circuits [72].

The phase of the input light can also be used, in addition to the polarization, to modulate SP propagation [71,73,74]. Fig. 2b shows a structure with two input terminals and two output terminals. By exciting SPs from the two input terminals I1 and I2 with coherent input light, two SP beams are generated. The two SP beams interfere and modulate the near-field distribution and far-field output signals depending on the phase difference of the two beams. Fig. 2bii–v shows the images for light routed to the O1 and O2 terminals, and the corresponding near-field distribution images. Based on the control of SP propagation, nanophotonic devices can be realized, for example plasmonic router, demultiplexer, switch, and Boolean logic gates [71–73].

Metal–dielectric composite nanostructures

Another class of composite nanostructures that are interesting for plasmonics are metal–dielectric composite structures. This is because SPs supported by the metal nanostructures are dependent on their dielectric environments, thus enabling control of the SPs by inducing changes to this environment. For example, increasing the refractive index of the dielectric surroundings leads to the red-shift of the SP resonance frequencies [20,75]. Such a local change in the environment can for example be induced by adsorption of molecules on the metal surface. This property has been used to develop surface plasmon resonance (SPR) sensor and localized surface plasmon resonance (LSPR) sensor for sensing and detection of chemical and biological molecules [20]. In larger particles, for example, Ag nanorice, multipolar resonances appear in the visible-light range, and longer particles show higher sensitivity to the change of the dielectric refractive index [76,77]. The dependence of the SP resonances on the dielectric environments makes the combination of metal and dielectric materials provide more tunability for the plasmonic properties.

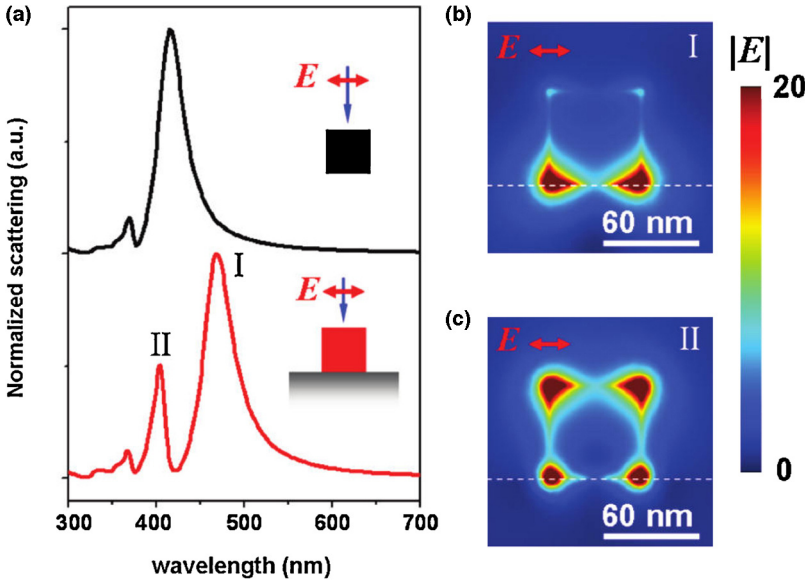

FIGURE 3

Ag nanocube–glass substrate composite structure. (a) Calculated scattering spectra of a 60 nm Ag cube in vacuum (black) and on a glass substrate (red), under normal incidence plane wave excitation. (b, c) Calculated electric field amplitude |E| distribution corresponding to peak I (469 nm) and peak II (404 nm), at a plane 1 nm away from the side surface of the cube. Dashed line represents the cube-substrate interface. Reproduced from Ref. [87].

Nanoparticle-based metal–dielectric composite systems

There are three main classes of nanoparticle-based metal–dielectric composite nanostructures: metal core–dielectric shell structures (hereafter denoted M/D structures), dielectric core–metal shell structures (hereafter D/M structures), and metal nanostructure–dielectric substrate coupled structures. The most typical M/D nanostructures are those formed by Au or Ag NPs coated with a dielectric layer of SiO_2. These M/D NPs are widely used for investigating plasmon-enhanced Raman scattering and fluorescence from molecular species attached to the NPs [78–81]. Coating the metal NPs with a dielectric layer prevents direct contact between the metal and the molecule to exclude the Raman signals from the metal–molecule interaction [82]. The thickness of the dielectric layer can strongly influence the fluorescence intensity of the emitters [83]. In contrast to M/D NPs, D/M NPs (called nanoshells in some papers) are obtained by coating a metal layer onto dielectric nanoparticles. The optical resonances of such composite D/M nanostructures can be tuned within the visible to near-infrared spectral range by controlling the ratio of the core diameter and the shell thickness [84]. One application that these D/M nanostructures has been used for is cancer therapy, whereby the photothermal effect in SiO_2/Au D/M NPs was employed [25,85].

Dielectric substrates can also dramatically affect the SPs in a nanostructure by breaking the symmetry of the environment [86,87]. Fig. 3a shows the scattering spectra of an Ag nanocube in vacuum and one placed on a glass substrate. For the cube–substrate composite nanostructure, the dipolar resonance peak (I) is red-shifted relative to that of the cube in vacuum, and a new peak (II) appears at 404 nm. The change of the scattering spectrum is caused by the substrate-mediated coupling of the dipolar and quadrupolar modes in the cube. The distributions of electric field amplitude for the two resonance wavelengths show different features (Figs. 3b,c). For the resonance peak of mode I at 469 nm, the electric field is localized on the substrate side. For the resonance peak of mode II at 404 nm, the electric field on the vacuum side is dominant. The resonance peak II shows an asymmetric line shape with a steeper slope at the large-wavelength-side of the peak (Fig. 3a), which is a Fano line-shape caused by the interference of the dipolar and quadrupolar modes. The influence of the substrate can be interpreted qualitatively by using an image-charge picture. As the magnitude of the induced charges in the substrate is dependent on the dielectric constant of the substrate, putting the cube on a substrate with larger dielectric constant will lead to larger energy shift of mode I and increased intensity ratio of mode II to mode I. The Fano resonance resulted from the coupling of the cube and the substrate contributes to larger LSPR sensitivity, which can be used for designing high-performance sensors.

Nanowire-based metal–dielectric composite systems

The dielectric materials can also strongly influence the propagating SPs on plasmonic nanowires. For Al_2O_3-coated Ag NWs on a glass substrate (Fig. 4a), the SP near-field distribution depends sensitively on the thickness of the dielectric Al_2O_3 layer, as well as the refractive index of the surrounding medium [88]. As seen from a comparison of the near-field distribution for three NWs of similar radius but with different Al_2O_3 thicknesses, the period of the near-field pattern increases from 1.7 to 5.8 μm when the Al_2O_3 thickness increases from 30 to 80 nm (Fig. 4b). Changing the refractive index of the surrounding dielectric material (air, water, oil in turn) dramatically changes the period of the near-field distribution (Fig. 4c)

In addition to dielectric coating, the substrate can also influence the propagating SPs on the Ag NWs. When an Ag NW is placed on a dielectric substrate, the oscillating charges of SP modes on the NW will couple to the induced charges in the substrate, which changes the original SP modes. The strength of this coupling between the NW and the substrate is dependent on the NW cross-section shape and refractive index of the substrate. It has been theoretically

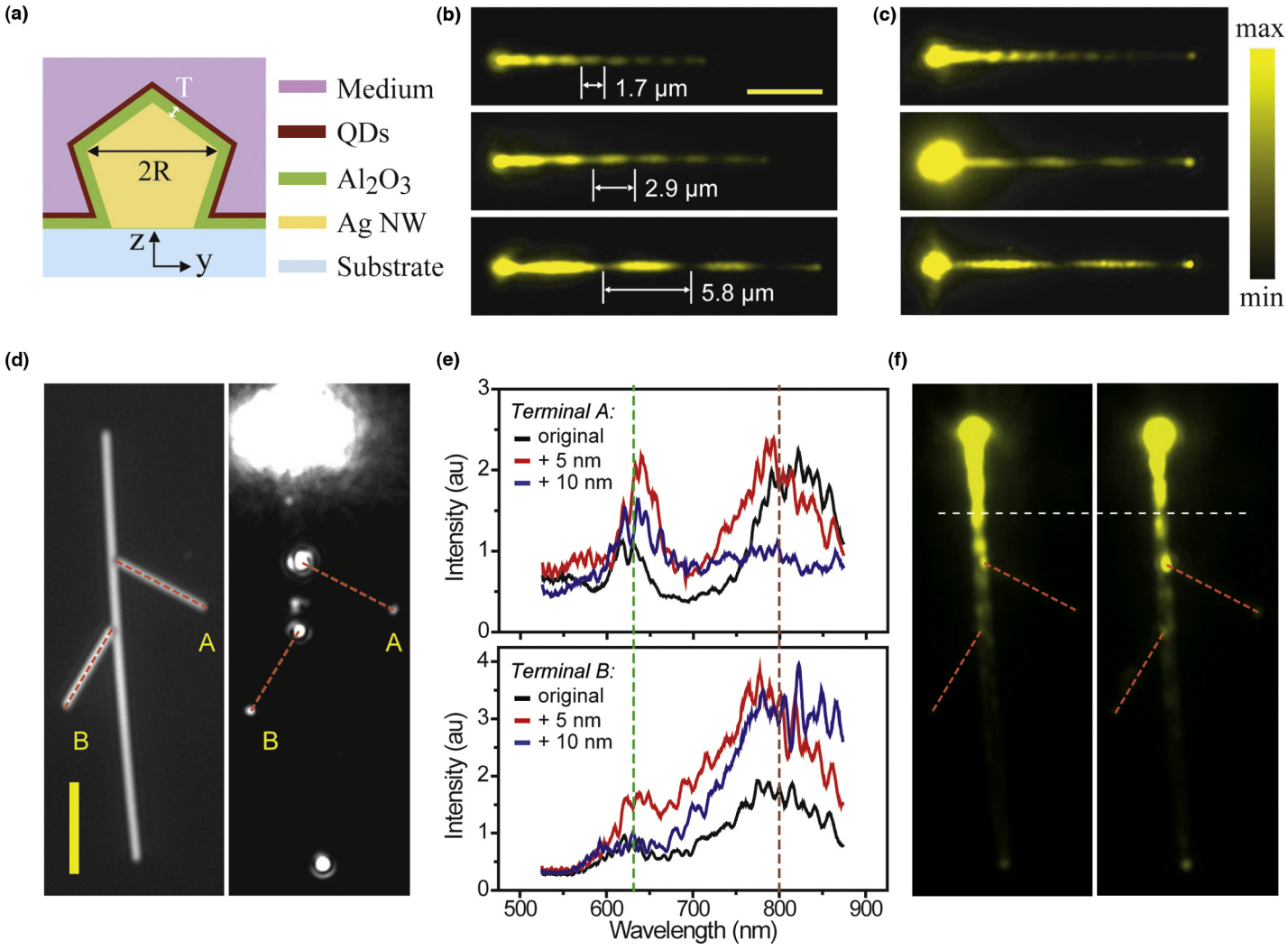

FIGURE 4

Controlling SP propagation in Al_2O_3-coated NWs on glass substrates by changing the thickness of the coating and dielectric environment. (a) Schematic cross-section of the NW samples. (b) QD fluorescence images indicating the near-field distribution under excitation at the left-hand ends of the NWs. The radius of the NWs is about 155 nm. From top to bottom, the corresponding Al_2O_3 thicknesses are 30, 50, and 80 nm. The scale bar represents 5 μm and applies to all images in (b) and (c). (c) QD emission images for a 155 nm radius NW initially coated with 10 nm of Al_2O_3 and QDs, and then capped with another 5 nm of Al_2O_3 to protect the water-soluble QDs from being removed, measured in air (top), water (middle), and oil (bottom). (d) A structure composed of three NWs was illuminated by supercontinuum light. The scale bar represents 5 μm. (e) The emission spectra at the terminal A (top) and B (bottom) for the original structure (black), and for 5 (red) and 10 nm (blue) Al_2O_3 layer deposited, respectively. (f) QD emission images when excited with a laser of 633 nm wavelength for the original structure (left) and after 5 nm more Al_2O_3 was deposited (right). Adapted from Ref. [88].

shown that, by using a thin high-refractive-index layer to separate the NW and the low-refractive-index substrate, the SP propagation loss due to leakage radiation can be decreased [89]. By depositing Al_2O_3 layer onto the Ag NW on glass substrate, the substrate-induced asymmetry is partly compensated. When the Al_2O_3 layer is thick enough, the NW feels a symmetric environment and the SP modes are equivalent to that for a NW embedded in glass matrix. Therefore, the thickness of the dielectric coating on the plasmonic waveguides, which can be precisely controlled by advanced film preparation techniques for example atomic layer deposition technique, can be used to tune the propagating SPs.

The ability to tune the propagation of SPs on NWs may enable the deterministic routing of SPs in a network of metal NWs. An example of such a network is composed of three Ag NWs on glass substrate (Fig. 4d), which are originally coated with Al_2O_3 of 30 nm thickness. The transmission spectra from the terminals of the two branches show the wavelength-dependent intensity (black lines in Fig. 4e). By adding 5 nm Al_2O_3 to the structure, the transmission spectra are changed (red lines in Fig. 4e). The intensity for most wavelengths is increased. By depositing additional 5 nm Al_2O_3, the spectra are changed further (blue lines in Fig. 4e). For terminal A, the spectral band of central wavelength about 633 nm (green dashed line in Fig. 4e) shows higher transmission intensity compared with other wavelengths. For terminal B, the longer wavelength light shows higher transmission intensity. The change of the transmission spectra with the Al_2O_3 coating is caused by the change of the near-field distributions. The near-field distribution images excited by 633 nm laser light (Fig. 4f) show that the near-field antinode is shifted to the junction for the right branch by depositing 5 nm Al_2O_3. This shift results in the increased transmission intensity at terminal A for 633 nm wavelength, which agrees well with the spectral results in Fig. 4e (black and red

intensity-curves at 633 nm for terminal A). These results demonstrate that the tunable near-field distribution controlled by the dielectric coating plays an important role in determining the SP propagating routes in plasmonic circuits.

Metal–semiconductor composite nanostructures

Semiconductor materials have many valuable optical and optoelectronic properties that can be modulated by the interaction between excitons and SPs [90]. It has been shown that coating Ag onto a CdS nanowire with a thin SiO_2 spacer layer leads to an enhancement of the radiative rate of excitons by more than 1000 times, and a decrease of the lifetime to the sub-picosecond range [91]. By encapsulating CdSe/ZnS QDs with an Au shell, the composite QD/Au nanoparticles preserve both fluorescent property of QDs and plasmonic property of Au shells, which could be useful for multimodal bioimaging [92]. Plasmon-enhanced absorption was observed in Au/PbS core–shell nanoparticles [93], and the plasmon-exciton interaction in Au/CdSe core–shell nanoparticles enables tailoring of the optical Stark effect and spin manipulation [94]. These studies demonstrate that the plasmon–exciton interaction can be used to modulate and design the optical properties of metal–semiconductor composite nanostructures.

The combination of metal and semiconductor also enables the realization of active plasmonic devices [95]. By coating a layer of CdSe QDs onto an Ag film, modulation of propagating SPs was demonstrated, which makes the composite system an all-optical

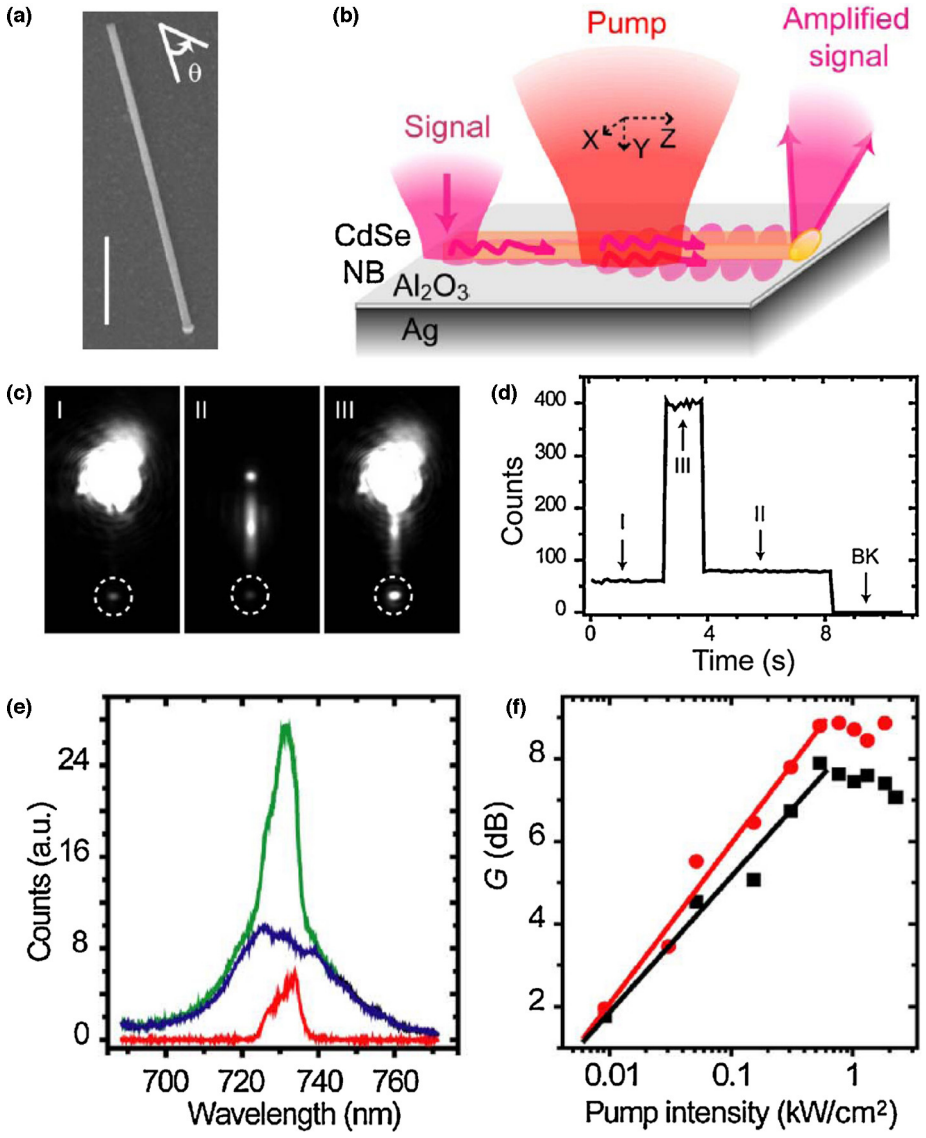

FIGURE 5

Loss-compensation of propagating SPs in a hybrid metal–dielectric–semiconductor system using an optical pump-probe scheme. (a) SEM image of a CdSe nanobelt deposited on the Al_2O_3-coated Ag film. The scale bar represents 2 μm. (b) Diagram of the excitation and amplification of input probe signal when operated in pump-probe setup. (c) Optical images obtained with 730 ± 5 nm band-pass filter, corresponding to a probe signal launched from the top end of the hybrid plasmonic waveguide and emitted from the bottom end highlighted by the dashed circle (I), photoluminescence (PL) with the pump only (II), and the amplification of the probe signal when both pump and probe are present (III). (d) Time trace of the output intensity at the emission end of the hybrid plasmonic waveguide. BK indicates the background dark counts. (e) Typical set of emission spectra, representing the probe signal (red), PL (blue), and amplified signal (green). (f) Gain G (dB) versus pump intensity for input laser beam polarized along (black) and perpendicular (red) to the waveguide. Adapted from Ref. [111].

modulator [96]. As the counterpart of laser, spaser (short for surface plasmon amplification by stimulated emission of radiation) was proposed as a nanoscale source of concentrated optical fields, in which semiconductor materials may be used as gain media [97,98]. Composite semiconductor nanostructure–metal film systems, for example CdS–MgF_2–Ag and InGaN/GaN–SiO_2–Ag, have been demonstrated to realize nanolasers with high mode confinement [99–101].

Semiconductor with high optical gain to compensate SP loss

Metallic (ohmic) losses inherent to plasmonic waveguides have hindered the development of plasmonic circuits. The possibility to compensate SP losses by use of gain media has been actively pursued experimentally and theoretically [102,103]. Many studies have been performed to compensate SP losses in metal film or metal strips by using dye molecules and fluorescent polymers as gain media [104–107]. Semiconductor quantum dots (QDs) have also been used as gain media to compensate SP losses by the interaction between SPs and semiconductor gain materials [108,109]. In a polymer-strip-loaded plasmonic waveguide doped with PbS QDs, an optical gain coefficient of 160 cm^{-1} was demonstrated at telecom wavelength [108]. It is experimentally demonstrated that the gain available for compensating the propagation loss of SPs may be limited by the amplified spontaneous emission of the QDs [109].

A particular system that has attracted attention because of its theoretical potential to confine optical modes to subwavelengths while minimizing propagation losses is based on a semiconductor–insulator–metal composite structure functioning as a hybrid plasmonic waveguide [110]. We demonstrated experimentally in a CdSe nanobelt–Al_2O_3–Ag hybrid plasmonic waveguide structure (Fig. 5a), the CdSe nanobelt can provide ultrahigh optical gain at room temperature to compensate the propagation loss of SPs [111]. The loss compensation was realized by using an optical pump-probe technique (Fig. 5b). The input probe signal was introduced into the waveguide via edge coupling at one end of the nanobelt (Fig. 5cI), and guided along the nanobelt with the electric field confined predominantly in the dielectric gap separating the semiconductor nanobelt from the metal film. By focusing pump light onto the CdSe nanobelt, the intensity of the probe signal measured at the output end of the hybrid system was found substantially amplified (Fig. 5c,d). The spectral measurements (Fig. 5e) show that the intensities of all wavelengths in the probe signal are amplified, demonstrating the broadband nature of the loss compensation scheme. High gain was achieved for inputs of both polarizations of along and perpendicular to the nanobelt, corresponding to transverse-magnetic (TM) and transverse-electric (TE) modes (Fig. 5f). The experimentally measured gain coefficients were 6140 cm^{-1} and 6755 cm^{-1} for TM and TE modes, respectively. The propagation loss of the TM mode is almost fully compensated by the gain. Compared with the CdSe nanobelt on a glass substrate, the gain in the hybrid plasmonic structure is much higher. Moreover, the plasmonic structure shows a much lower transparency pump intensity which indicates the start of gain. The loss compensation by pumping the gain materials can significantly increase the propagation length of the signal in plasmonic devices, which will promote the development of plasmonic circuits for information technologies.

Summary and outlook

We have highlighted a few typical plasmonic composite nanostructures here. Composite nanostructures indeed play key roles in plasmonics in terms of tuning optical properties and enabling various potential applications. Metal–metal coupled nanostructures give a large electromagnetic field enhancement, which is the basic property used in many plasmonics-related areas. Metal–dielectric composite nanostructures make the plasmonic properties more tunable because of the dependence of SPs on the metal's dielectric environment. In metal–semiconductor composite nanostructures, optical properties can be tuned by the interactions between plasmons and excitons, and active plasmonic devices can be designed.

Nanostructure engineering with improved control abilities and rational design strategies will promote the further developments of various composite plasmonic structures and devices for applications in different fields. The composite metal–biomaterial nanostructures may greatly benefit the bio-applications of plasmonics, for example biological sensing and imaging, and medical diagnostics. Metal–graphene composite nanostructures can open new directions in the fields of, for example sensing and optoelectronics, to combine the benefits of the plasmonics and graphene fields. Recent studies have clearly shown the metal–graphene composite systems can improve the performances of metal nanostructures for SERS and of graphene photodetectors [112–114]. By combining metal nanostructures with nonlinear, optoelectronic, electro-optic and other functional materials, plasmonic devices with outstanding performances can be expected, which will promote the development of plasmonic circuitry for a new generation of information technology. Moreover, new phenomena and new sciences arising from the interaction of plasmons and the specific materials may be found in these new composite systems.

Acknowledgements

This work was supported by National Natural Science Foundation of China (Grant Nos. 11134013, 11227407, 11374012 and 61210017), The Ministry of Science and Technology of the People's Republic of China (Grant No. 2012YQ12006005), Knowledge Innovation Project (Grant No. KJCX2-EW-W04) and Youth Innovation Promotion Association of Chinese Academy of Sciences.

References

[1] W.L. Barnes, et al. Nature 424 (2003) 824–830.
[2] J.B. Pendry, et al. Science 305 (2004) 847–848.
[3] C.R. Williams, et al. Nat. Photon. 2 (2008) 175–179.
[4] Q. Feng, et al. Opt. Lett. 37 (2012) 2133–2135.
[5] B. Ng, et al. Adv. Opt. Mater. 1 (2013) 543–548.
[6] A.P. Hibbins, et al. Science 308 (2005) 670–672.
[7] H.X. Xu, et al. Phys. Rev. Lett. 83 (1999) 4357–4360.
[8] H.X. Xu, et al. Phys. Rev. E 62 (2000) 4318–4324.
[9] L.M. Tong, et al. Phys. Chem. Chem. Phys. 15 (2013) 4100–4109.
[10] H. Wei, H.X. Xu, Nanoscale 5 (2013) 10794–10805.
[11] T. Shegai, et al. Proc. Natl. Acad. Sci. U. S. A. 105 (2008) 16448–16453.
[12] Z.P. Li, et al. ACS Nano 3 (2009) 637–642.
[13] H.X. Xu, M. Kall, Phys. Rev. Lett. 89 (2002) 246802.
[14] F. Svedberg, et al. Nano Lett. 6 (2006) 2639–2641.
[15] M.T. Sun, et al. Sci. Rep. 2 (2012) 647.
[16] L. Mao, et al. Appl. Phys. Lett. 94 (2009) 243102.
[17] K.J. Savage, et al. Nature 491 (2012) 574–577.
[18] P. Muhlschlegel, et al. Science 308 (2005) 1607–1609.

[19] S. Kim, et al. Nature 453 (2008) 757–760.
[20] K.M. Mayer, J.H. Hafner, Chem. Rev. 111 (2011) 3828–3857.
[21] D.K. Gramotnev, S.I. Bozhevolnyi, Nat. Photon. 4 (2010) 83–91.
[22] H. Wei, H.X. Xu, Nanophotonics 1 (2012) 155–169.
[23] X.H. Huang, et al. Nano Lett. 7 (2007) 1591–1597.
[24] X.M. Qian, et al. Nat. Biotechnol. 26 (2008) 83–90.
[25] R. Bardhan, et al. Acc. Chem. Res. 44 (2011) 936–946.
[26] E. Ozbay, Science 311 (2006) 189–193.
[27] R.W. Heeres, et al. Nat. Nanotechnol. 8 (2013) 719–722.
[28] H.A. Atwater, A. Polman, Nat. Mater. 9 (2010) 205–213.
[29] S. Linic, et al. Nat. Mater. 10 (2011) 911–921.
[30] M.T. Sun, H.X. Xu, Small 8 (2012) 2777–2786.
[31] X.G. Luo, T. Ishihara, Appl. Phys. Lett. 84 (2004) 4780–4782.
[32] Z.W. Liu, et al. Nano Lett. 5 (2005) 957–961.
[33] X. Zhang, Z. Liu, Nat. Mater. 7 (2008) 435–441.
[34] H.X. Xu, J. Quant. Spectrosc. Radiat. Trans. 87 (2004) 53–67.
[35] J. Zuloaga, et al. Nano Lett. 9 (2009) 887–891.
[36] R. Esteban, et al. Nat. Commun. 3 (2012) 825.
[37] H.X. Xu, et al. Phys. Rev. Lett. 93 (2004) 243002.
[38] O.L. Muskens, et al. Nano Lett. 7 (2007) 2871–2875.
[39] M. Ringler, et al. Phys. Rev. Lett. 100 (2008) 203002.
[40] M. Danckwerts, L. Novotny, Phys. Rev. Lett. 98 (2007) 026104.
[41] J.Y. Suh, et al. Nano Lett. 12 (2012) 5769–5774.
[42] Z.P. Li, et al. Phys. Rev. B 77 (2008) 085412.
[43] L.M. Tong, et al. Nano Lett. 11 (2011) 4505–4508.
[44] M.L. Juan, et al. Nat. Photon. 5 (2011) 349–356.
[45] T. Shegai, et al. Acs Nano 5 (2011) 2036–2041.
[46] A.G. Curto, et al. Science 329 (2010) 930–933.
[47] M. Rycenga, et al. Chem. Rev. 111 (2011) 3669–3712.
[48] S. Sheikholeslami, et al. Nano Lett. 10 (2010) 2655–2660.
[49] T. Shegai, et al. Nat. Commun. 2 (2011) 481.
[50] A.M. Funston, et al. Nano Lett. 9 (2009) 1651–1658.
[51] F. Shafiei, et al. Nat. Photon. 7 (2013) 367–372.
[52] B. Luk'yanchuk, et al. Nat. Mater. 9 (2010) 707–715.
[53] S. Zhang, et al. Phys. Rev. Lett. 101 (2008) 047401.
[54] N. Liu, et al. Nat. Mater. 8 (2009) 758–762.
[55] H.X. Xu, M. Kall, ChemPhysChem 4 (2003) 1001–1005.
[56] H. Wei, et al. Small 4 (2008) 1296–1300.
[57] H. Wei, et al. Nano Lett. 8 (2008) 2497–2502.
[58] Y.R. Fang, et al. Nano Lett. 9 (2009) 2049–2053.
[59] S. Mubeen, et al. Nano Lett. 12 (2012) 2088–2094.
[60] J.N. Chen, et al. Appl. Phys. Lett. 92 (2008) 093110.
[61] Z.L. Yang, et al. J. Raman Spectrosc. 40 (2009) 1343–1348.
[62] K. Uetsuki, et al. Nanoscale 4 (2012) 5931–5935.
[63] R. Zhang, et al. Nature 498 (2013) 82–86.
[64] J.C. Weeber, et al. Phys. Rev. B 64 (2001) 045411.
[65] S.I. Bozhevolnyi, et al. Nature 440 (2006) 508–511.
[66] J.A. Dionne, et al. Nano Lett. 6 (2006) 1928–1932.
[67] H. Ditlbacher, et al. Phys. Rev. Lett. 95 (2005) 257403.
[68] P. Kusar, et al. Nano Lett. 12 (2012) 661–665.
[69] Z.X. Wang, et al. Laser Photon. Rev. (2014), http://dx.doi.org/10.1002/lpor.201300215.
[70] H. Wei, et al. Nano Lett. 9 (2009) 4168–4171.
[71] H. Wei, et al. Nano Lett. 11 (2011) 471–475.
[72] Y.R. Fang, et al. Nano Lett. 10 (2010) 1950–1954.
[73] H. Wei, et al. Nat. Commun. 2 (2011) 387.
[74] H. Wei, H.X. Xu, Nanoscale 4 (2012) 7149–7154.
[75] H.X. Xu, M. Kall, Sens. Actuator B Chem. 87 (2002) 244–249.
[76] H. Wei, et al. Acs Nano 4 (2010) 2649–2654.
[77] H.Y. Liang, et al. Chem. Mater. 24 (2012) 2339–2346.
[78] W. Wang, et al. Acs Nano 3 (2009) 3493–3496.
[79] H.X. Xu, Appl. Phys. Lett. 85 (2004) 5980–5982.
[80] K. Aslan, et al. J. Am. Chem. Soc. 129 (2007) 1524–1525.
[81] T. Ming, et al. Nano Lett. 9 (2009) 3896–3903.
[82] J.F. Li, et al. Nature 464 (2010) 392–395.
[83] F. Zhang, et al. J. Am. Chem. Soc. 132 (2010) 2850–2851.
[84] S.J. Oldenburg, et al. Chem. Phys. Lett. 288 (1998) 243–247.
[85] L.R. Hirsch, et al. Proc. Natl. Acad. Sci. U. S. A. 100 (2003) 13549–13554.
[86] M.W. Knight, et al. Nano Lett. 9 (2009) 2188–2192.
[87] S.P. Zhang, et al. Nano Lett. 11 (2011) 1657–1663.
[88] H. Wei, et al. Proc. Natl. Acad. Sci. U. S. A. 110 (2013) 4494–4499.
[89] S.P. Zhang, H.X. Xu, Acs Nano 6 (2012) 8128–8135.
[90] M. Achermann, J. Phys. Chem. Lett. 1 (2010) 2837–2843.
[91] C.H. Cho, et al. Nat. Mater. 10 (2011) 669–675.
[92] Y.D. Jin, X.H. Gao, Nat. Nanotechnol. 4 (2009) 571–576.
[93] J.S. Lee, et al. J. Am. Chem. Soc. 130 (2008) 9673–9675.
[94] J.T. Zhang, et al. Nature 466 (2010) 91–95.
[95] O. Hess, et al. Nat. Mater. 11 (2012) 573–584.
[96] D. Pacifici, et al. Nat. Photon. 1 (2007) 402–406.
[97] D.J. Bergman, M.I. Stockman, Phys. Rev. Lett. 90 (2003) 027402.
[98] M.I. Stockman, Nat. Photon. 2 (2008) 327–329.
[99] R.F. Oulton, et al. Nature 461 (2009) 629–632.
[100] R.M. Ma, et al. Nat. Mater. 10 (2011) 110–113.
[101] Y.J. Lu, et al. Science 337 (2012) 450–453.
[102] P. Berini, I. De Leon, Nat. Photon. 6 (2012) 16–24.
[103] G.C. des Francs, et al. Opt. Exp. 18 (2010) 16327–16334.
[104] J. Seidel, et al. Phys. Rev. Lett. 94 (2005) 177401.
[105] M.A. Noginov, et al. Phys. Rev. Lett. 101 (2008) 226806.
[106] I. De Leon, P. Berini, Nat. Photon. 4 (2010) 382–387.
[107] M.C. Gather, et al. Nat. Photon. 4 (2010) 457–461.
[108] J. Grandidier, et al. Nano Lett. 9 (2009) 2935–2939.
[109] P.M. Bolger, et al. Opt. Lett. 35 (2010) 1197–1199.
[110] R.F. Oulton, et al. Nat. Photon. 2 (2008) 496–500.
[111] N. Liu, et al. Sci. Rep. 3 (2013) 1967.
[112] W.G. Xu, et al. Proc. Natl. Acad. Sci. U. S. A. 109 (2012) 9281–9286.
[113] T.J. Echtermeyer, et al. Nat. Commun. 2 (2011) 458.
[114] Y. Liu, et al. Nat. Commun. 2 (2011) 579.